Journal of Sound and Vibration 472 (2020) 115203

Contents lists available at ScienceDirect

Journal of Sound and Vibration

journal homepage: www.elsevier.com/locate/jsvi

Rapid Communications

Hyperchaos co-existing with periodic orbits in a frictional oscillator

Merten Stender [a,*], Martin Jahn [b], Norbert Hoffmann [a,c], Jörg Wallaschek [b]

[a] Dynamics Group, Hamburg University of Technology, Hamburg, Germany
[b] Institute of Dynamics and Vibration Research, Leibniz Universität Hannover, Hannover, Germany
[c] Department of Mechanical Engineering, Imperial College London, London, United Kingdom

ARTICLE INFO

Article history:
Received 25 November 2019
Revised 9 January 2020
Accepted 18 January 2020
Available online 23 January 2020
Handling Editor: A.V. Metrikine

Keywords:
Nonlinear dynamics
Friction-induced vibrations
Mode-coupling
Chaos
Multi-stability

ABSTRACT

This work reports observations of complex dynamical behavior and chimera-alike dynamics in a self-excited frictional oscillator with a weak stiffness nonlinearity. Multi-stability in the form of several co-existing stable limit cycle solutions are identified for a wide range of system parameters. For a particular system configuration, an unstable periodic orbit is found that gives rise to irregular long-term behavior. Trajectories starting from this orbit turn out to be hyper-chaotic with multiple positive Lyapunov exponents. Trajectories starting from different regions in phase space converge to stable limit cycles. Hence, this numerical study reveals co-existing regular and irregular dynamics at a fixed system configuration. This sensitive dependence of the qualitative system dynamics on initial conditions adds new aspects to a better understanding of the rich dynamic behavior of structures subjected to friction-induced vibrations.

1. Introduction

Even today, the numerical prediction of vibrations in real-world mechanical systems remains challenging such that one may claim that predictive models for a range of systems, including those affected by friction, are still missing [1]. Owing to nonlinearities, dynamic systems of this type can exhibit sensitive dependence on initial conditions, that give rise to multiple solutions or chaotic dynamics. Besides uncertain model geometries, contact conditions [2] and component properties, the exact knowledge about the initial conditions is missing in most cases. Often, and driven by intuition, a frictional system is assumed to exhibit a single and unique response for a fixed parameter configuration or a given external load. However, in a multi-stability scenario [3], i.e. a fixed system configuration that exhibits multiple steady-state responses, only the choice of initial conditions and the consideration of instantaneous perturbations dictate the resulting dynamics. Recently, phenomena of multi-stability and localization were shown to exist in a chain of identical friction-excited oscillators [4], while chaos in frictional systems was reported by Ref. [5] and shown experimentally by Refs. [6,7] amongst others. This work illustrates the appearance of a multi-faced dynamical behavior in a simple frictional oscillator with steady sliding. Particularly, the emergence of periodic and chaotic motions are shown to depend solely on the initial conditions. The dynamical system studied in this work is introduced first. Then, multiplicity of periodic solutions is presented. Finally, hyperchaotic motion existing in parallel to limit cycle solutions is depicted, which reminds us of chimera states in coupled oscillators.

* Corresponding author.
E-mail address: m.stender@tuhh.de (M. Stender).
URL: http://www.tuhh.de/dyn (M. Stender).

https://doi.org/10.1016/j.jsv.2020.115203
0022-460X/

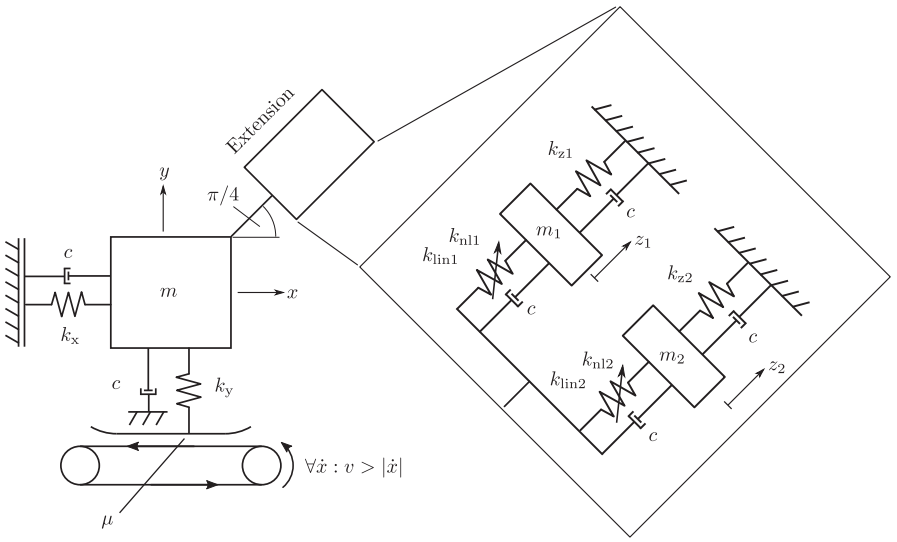

Fig. 1. Friction oscillator from Ref. [8] and extended by a two-mass linear subsystem connected to the slider by weakly nonlinear (cubic) stiffnesses k_{nl}. Reference parameters that were studied in previous works [9,10]: $\mu = 0.65, m = 1\,\text{kg}, k_x = 11\,\frac{\text{N}}{\text{m}}, k_y = 20\,\frac{\text{N}}{\text{m}}, k_{z1} = 100\,\frac{\text{N}}{\text{m}}, k_{z2} = 20\,\frac{\text{N}}{\text{m}}, k_{lin1,2} = 10\,\frac{\text{N}}{\text{m}}, k_{nl1,2} = 5\,\frac{\text{N}}{\text{m}}, c = 0.02\,\frac{\text{Ns}}{\text{m}}$, equations of motion given in Appendix A.

2. Frictional oscillator

We are studying the dynamic system [8] in Fig. 1 that comprises a sliding mass and a linear two-mass subsystem which are connected through a nonlinear joint [9] as recently proposed in Ref. [10]. The horizontal and vertical motions of the slider are viscously damped and coupled through the inclined stiffness and the frictional contact. The speed of the conveyor belt is assumed to always be larger than the horizontal velocity of the sliding mass such that the system is not undergoing any stick-slip type dynamics. Coulomb friction is implemented as the friction law. The nonlinear joint, representing the only nonlinear component in the system, is implemented as a weak cubic stiffness nonlinearity. The symmetry in the subsystem is broken by different choices for the stiffness k_z.

The system exhibits self-excited vibrations through mode-coupling instabilities [8]. In Ref. [9] the authors show the rich bifurcation behavior of a smaller model that comprises a single-mass subsystem. In the following, we study the bifurcations of different nonlinear solutions along the variation of the tangential stiffness k_x utilizing the orthogonal collocation based continuation package MATCONT [11]. Appropriate initial solutions, including those on detached branches, have been determined using inhouse code at IDS that features the extended periodic motion concept within the harmonic balance method and a predictor-corrector scheme as proposed in Ref. [10]. 15 harmonics have been included within the HBM for computation of initial solutions at constant values of k_x.

3. Multiple co-existing regular solutions

Fig. 2 (a) displays the bifurcation diagram for the oscillator in the reference damping configuration. For increasing stiffness k_x, the equilibrium EP loses stability at $k_x \approx 7\,\frac{\text{N}}{\text{m}}$. The limit cycle LC1 arises through a subcritical Hopf bifurcation and grows steeply to large amplitudes. For larger stiffness values, the limit cycle connects to a second Hopf point at $k_x \approx 24\,\frac{\text{N}}{\text{m}}$. Above this stiffness value, several periodic solutions exist parallel to a stable fixed point. Here, potentially dangerous jumping phenomena may occur when the equilibrium is perturbed and the system jumps to a high-amplitude limit cycle solution. Further, an isola, i.e. a limit cycle without connection to other solution branches, co-exists with the first limit cycle for $k_x > 10.5\,\frac{\text{N}}{\text{m}}$. The isola folds twice, as depicted in the detail view, such that for a short parameter range there exist five limit cycles in parallel. The five limit cycles LC1 to LC5 are enumerated by their maximum horizontal displacement in x.

In Fig. 2 (b) the state space of the six co-existing solutions of the system are displayed for the stiffness value $k_x = 11.2\,\frac{\text{N}}{\text{m}}$. In this multi-stability scenario, the steady-state response amplitude may vary significantly, e.g. between LC1 and LC4, depending on the initial conditions.

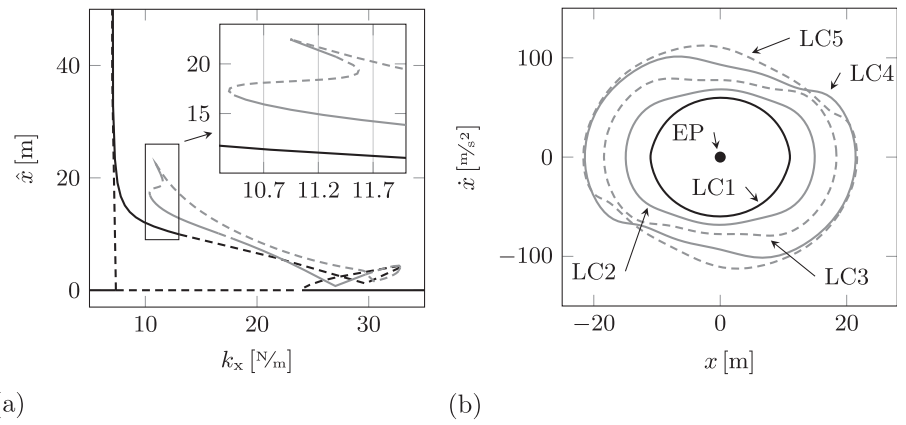

Fig. 2. Reference damping $c = 0.02\frac{\text{Ns}}{\text{m}}$: (a) bifurcation diagram for the horizontal stiffness k_x. (b) state space of the horizontal motion and the solutions co-existing at $k_x = 11.2\,\frac{\text{N}}{\text{m}}$. The isola solutions as displayed in gray color, stable and unstable solutions are depicted by solid and dashed lines, respectively. Amplitudes are reported as the steady state maximum horizontal displacement along one period of each limit cycle, i.e. $\hat{x} = \max\left(x\left(t_1 \le t \le t_1 + \frac{2\pi}{\Omega}\right)\right)$, where Ω is the frequency of vibration.

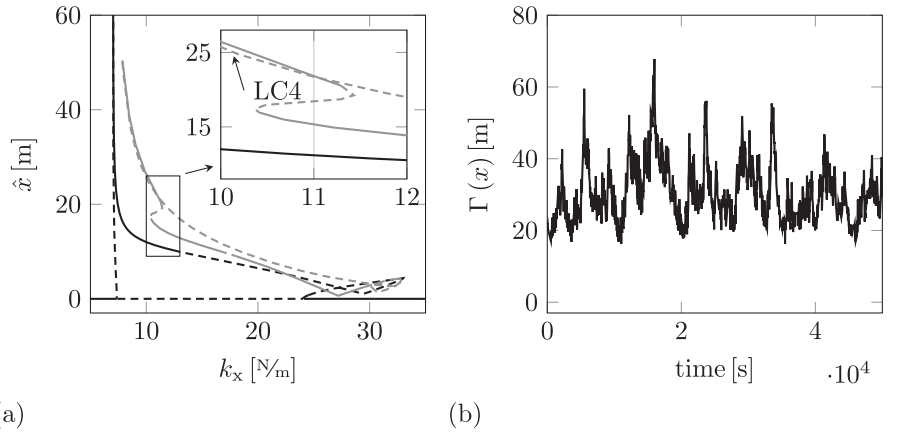

Fig. 3. Reduced damping $c = 0.002\frac{\text{Ns}}{\text{m}}$ configuration: (a) bifurcation diagram for the horizontal stiffness k_x where the isola branches are displayed in gray color. (b) time evolution of the first state's local maxima $\Gamma(x)$ starting from the unstable limit cycle LC4 at $k_x = 11.0\,\frac{\text{N}}{\text{m}}$. Initial conditions are given in Appendix B.

4. Co-existing regular and hyperchaotic solutions

To complement the picture and replicate the situation in real-world structures where damping is difficult to determine, frequency-dependent and subjected to fluctuations [9], a reduced damping level of $c = 0.002\frac{\text{Ns}}{\text{m}}$ is studied. While the bifurcation behavior of the first limit cycle connected to the Hopf points remains similar, the detached limit cycle shows a more complicated branching behavior towards smaller bifurcation parameter values in Fig. 3 (a) The recurring character of intertwining solution branches, especially observed in the region of the second Hopf bifurcation at larger stiffness values around $24 \le k_x \le 32\,\frac{\text{N}}{\text{m}}$, somewhat resemble the snaking patterns observed for nonlinear localization in coupled oscillator chains [4]. During the study, it has been observed that trajectories starting from initial conditions close to the unstable periodic orbit LC4 at $k_x = 11.0\,\frac{\text{N}}{\text{m}}$ do not converge to one of the neighboring stable limit cycles. Instead, irregular long-term behavior in the form of a-periodicity and strongly modulating vibration amplitudes can be observed. The upper envelope $\Gamma(x)$, i.e. the local maxima of the horizontal motion, is not constant as it would be in the case of a periodic motion, but is highly irregular as depicted in Fig. 3 (b). Extensive numerical experiments involving different time marching schemes and very long observation times provide evidence for ruling out transient chaos here.

To characterize the irregular motion, the Lyapunov spectrum was determined using a semi-analytical variational approach along with the time integration to observe the divergence of instantaneous perturbations along the trajectories. The Lyapunov spectrum is given by

$$\Lambda = [0.381, 0.213, 0.075, -00001, -0.002, -0.079, -0.218 - 0.386]^{\top} \tag{1}$$

which indicates that the irregular motion is in fact hyperchaotic. There are at least three positive Lyapunov exponents, which fulfills the condition of hyperchaos, stating that there are at least two positive exponents. Trajectories starting from the other unstable periodic orbit converge to one of the stable limit cycles.

Thus, solely depending on the initial conditions, there is the possibility of ending up on three different stable periodic orbits or on an irregular motion in this configuration. Such behavior can be expected for conservative and weakly damped systems taking into account the plethora of localized and chaotic solutions of cyclically coupled oscillators. However, and to the knowledge of the authors, such multiplicity of regular and irregular solutions has not yet been reported in models of friction-excited oscillators without cyclic symmetry. In fact, such an observation contradicts the typical notion of an oscillator being either *periodic* or *chaotic*. The presented oscillator is both at the same time, solely depending on the choice of initial conditions - much like the famous chimera states in coupled oscillators.

Hence, if a rather simple analytical model is capable of showing such multi-faced and complicated dynamics, one must assume even more complex dynamics to exist in realistic systems involving many components and multiple nonlinearities. What if the seemingly random or elusive emergence of friction-induced vibrations in experiments and the missing repeatability in the system response at seemingly constant laboratory conditions is just an expression of such chimera-alike system properties? In future work, the basins of attraction, possible links to snaking phenomena and the characteristics of the chaotic motion will be studied in detail.

5. Conclusion

We present preliminary results on a weakly nonlinear frictional oscillator that exhibits both regular and chaotic solutions for a fixed system configuration. In a particular configuration, trajectories on an unstable periodic orbit were identified that initiate hyperchaotic long-term behavior, while trajectories starting from other phase space regions settled to periodic orbits. Thus, the qualitative dynamic behavior in terms of regularity and irregularity solely depends on the choice of initial conditions here. Hence, this rather simple oscillator can appear periodic and chaotic at the same time. Such a system behavior may be one aspect for explaining elusive friction-induced vibrations as observed in experiments and the limited prediction quality of state-of-the-art numerical simulations for realistic mechanical systems affected by friction.

Author contributions

All authors designed the research and discussed the results. MS and MJ performed the research and created the artwork, MS wrote the manuscript.

CRediT authorship contribution statement

Merten Stender: Conceptualization, Methodology, Formal analysis, Visualization, Writing - original draft. **Martin Jahn:** Conceptualization, Methodology, Formal analysis, Validation, Writing - review & editing. **Norbert Hoffmann:** Conceptualization, Supervision, Writing - review & editing. **Jörg Wallaschek:** Conceptualization, Supervision, Writing - review & editing.

Acknowledgment

M.S. was supported by the German Research Foundation (DFG) within the Priority Program"'calm, smooth, smart"' under the reference Ho 3851/12-1. M.J. was supported by the German Research Foundation (DFG) within the Priority Program"'calm, smooth, smart"' under the reference PA 846/5-1 and WA 564/37-1.

Appendix A. Equations of motion

$$
\begin{bmatrix} m & 0 & 0 & 0 \\ 0 & m & 0 & 0 \\ 0 & 0 & m_1 & 0 \\ 0 & 0 & 0 & m_2 \end{bmatrix} \begin{bmatrix} \ddot{x} \\ \ddot{y} \\ \ddot{z}_1 \\ \ddot{z}_2 \end{bmatrix}
+ \begin{bmatrix} 2c & c & -\frac{c}{\sqrt{2}} & -\frac{c}{\sqrt{2}} \\ c & 2c & -\frac{c}{\sqrt{2}} & -\frac{c}{\sqrt{2}} \\ -\frac{c}{\sqrt{2}} & -\frac{c}{\sqrt{2}} & 2c & 0 \\ -\frac{c}{\sqrt{2}} & -\frac{c}{\sqrt{2}} & 0 & 2c \end{bmatrix} \begin{bmatrix} \dot{x} \\ \dot{y} \\ \dot{z}_1 \\ \dot{z}_2 \end{bmatrix}
$$

$$
+ \begin{bmatrix} k_x + \frac{k_{lin1}}{2} + \frac{k_{lin2}}{2} & \frac{k_{lin1}}{2} + \frac{k_{lin2}}{2} - \mu k_y & -\frac{k_{lin1}}{\sqrt{2}} & -\frac{k_{lin2}}{\sqrt{2}} \\ \frac{k_{lin1}}{2} + \frac{k_{lin2}}{2} & k_y + \frac{k_{lin1}}{2} + \frac{k_{lin2}}{2} & -\frac{k_{lin1}}{\sqrt{2}} & -\frac{k_{lin2}}{\sqrt{2}} \\ -\frac{k_{lin1}}{\sqrt{2}} & -\frac{k_{lin1}}{\sqrt{2}} & k_{z1} + k_{lin1} & 0 \\ -\frac{k_{lin2}}{\sqrt{2}} & -\frac{k_{lin2}}{\sqrt{2}} & 0 & k_{z2} + k_{lin2} \end{bmatrix} \begin{bmatrix} x \\ y \\ z_1 \\ z_2 \end{bmatrix}
$$

$$
+ \begin{bmatrix} -\frac{1}{\sqrt{2}} & -\frac{1}{\sqrt{2}} \\ -\frac{1}{\sqrt{2}} & -\frac{1}{\sqrt{2}} \\ 1 & 0 \\ 0 & 1 \end{bmatrix} \begin{bmatrix} k_{nl1}\left(z_1 - \frac{(x+y)}{\sqrt{2}} \right)^3 \\ k_{nl2}\left(z_2 - \frac{(x+y)}{\sqrt{2}} \right)^3 \end{bmatrix} = \mathbf{0} \tag{A.1}
$$

Appendix B. Initial conditions on periodic orbits

Initial conditions at $k_x = 11.2 \frac{N}{m}$ for $c = 0.02 \frac{Ns}{m}$:

$\mathbf{x}_{LC1} = [10.97, -17.27, -0.72, -5.12, -3.93, 7.47, -2.16, 0.58]^\top$

$\mathbf{x}_{LC2} = [14.89, -21.84, -3.11, -6.89, 7.44, -6.20, -6.70, -5.36]^\top$

$\mathbf{x}_{LC3} = [18.32, -22.30, -3.12, -4.42, 8.41, -3.22, -11.36, -3.86]^\top$

$\mathbf{x}_{LC4} = [21.39, -23.98, -2.77, -3.10, 6.12, 7.91, -20.45, -3.18]^\top$

$\mathbf{x}_{LC5} = [18.75, -19.89, -3.26, -2.46, -57.67, 65.36, 1.48, 5.33]^\top$

Initial conditions at $k_x = 11.0 \frac{N}{m}$ for $c = 0.002 \frac{Ns}{m}$:

$\mathbf{x}_{LC1} = [11.17, -17.37, -0.69, -5.04, -0.36, 0.58, -0.14, 0.03]^\top$

$\mathbf{x}_{LC2} = [15.29, -21.98, -3.12, -6.73, -1.72, 1.61, 0.76, 0.50]^\top$

$\mathbf{x}_{LC3} = [18.42, -22.45, -3.26, -4.58, -1.97, 1.85, 0.66, 0.32]^\top$

$\mathbf{x}_{LC4} = [12.93, -12.63, -2.86, -1.37, -92.67, 101.32, 7.16, 9.02]^\top$

$\mathbf{x}_{LC5} = [21.85, -24.11, -3.39, -3.25, -2.52, 2.84, 0.01, 0.20]^\top$

References

[1] T. Butlin, J. Woodhouse, Sensitivity of friction-induced vibration in idealised systems, J. Sound Vib. 319 (12) (2009) 182–198, https://doi.org/10.1016/j.jsv.2008.05.034 2009.

[2] E. Denimal, J.-J. Sinou, S. Nacivet, L. Nechak, Squeal analysis based on the effect and determination of the most influential contacts between the different components of an automotive brake system, Int. J. Mech. Sci. 151 (2019) 192–213, https://doi.org/10.1016/j.ijmecsci.2018.10.054 2019.

[3] D. Dudkowski, S. Jafari, T. Kapitaniak, N.V. Kuznetsov, G.A. Leonov, A. Prasad, Hidden attractors in dynamical systems, Phys. Rep. 637 (2016) 1–50, https://doi.org/10.1016/j.physrep.2016.05.002 2016.

[4] A. Papangelo, N. Hoffmann, A. Grolet, M. Stender, M. Ciavarella, Multiple spatially localized dynamical states in friction-excited oscillator chains, J. Sound Vib. 417 (2018) 56–64, https://doi.org/10.1016/j.jsv.2017.11.056 2018.

[5] J. Awrejcewicz, Chaos in simple mechanical systems with friction, J. Sound Vib. 109 (1) (1986) 178–180, https://doi.org/10.1016/S0022-460X(86)80032-3 1986.

[6] S. Oberst, J. Lai, Chaos in brake squeal noise, J. Sound Vib. 330 (5) (2011) 955–975, https://doi.org/10.1016/j.jsv.2010.09.009 2011.

[7] V. Pilipchuk, P. Olejnik, J. Awrejcewicz, Transient friction-induced vibrations in a 2-dof model of brakes, J. Sound Vib. 344 (2015) 297–312, https://doi.org/10.1016/j.jsv.2015.01.028 2015.

[8] N. Hoffmann, M. Fischer, R. Allgaier, L. Gaul, A minimal model for studying properties of the mode-coupling type instability in friction induced oscillations, Mech. Res. Commun. 29 (4) (2002) 197–205, https://doi.org/10.1016/S0093-6413(02)00254-9 2002.

[9] S. Kruse, M. Tiedemann, B. Zeumer, P. Reuss, H. Hetzler, N. Hoffmann, The influence of joints on friction induced vibration in brake squeal, J. Sound Vib. 340 (2015) 239–252, https://doi.org/10.1016/j.jsv.2014.11.016 2015.

[10] M. Jahn, M. Stender, S. Tatzko, N. Hoffmann, A. Grolet, J. Wallaschek, The extended periodic motion concept for fast limit cycle detection of self-excited systems, Comput. Struct. (2019) 106139, https://doi.org/10.1016/j.compstruc.2019.106139 2019.

[11] A. Dhooge, W. Govaerts, Y.A. Kuznetsov, Matcont, ACM Transactions on Mathematical Software 29 (2) (2003) 141–164, https://doi.org/10.1145/779359.779362 2003.